BJ www.biochemj.org

BJ Plant

Biochem. J. (2012) **445**, 101–111 (Printed in Great Britain) doi:10.1042/BJ20111704

online data

A conserved cysteine residue is involved in disulfide bond formation between plant plasma membrane aquaporin monomers

Gerd P. BIENERT*[1], Damien CAVEZ*[1], Arnaud BESSERER*, Marie C. BERNY*, Dimitri GILIS†, Marianne ROOMAN† and François CHAUMONT*[2]

*Institut des Sciences de la Vie, Université Catholique de Louvain, Croix du Sud, 4-L7.07.14, 1348 Louvain-la-Neuve, Belgium, and †Bioinformatique génomique et structurale, Université Libre de Bruxelles, 1050 Brussels, Belgium

AQPs (aquaporins) are conserved in all kingdoms of life and facilitate the rapid diffusion of water and/or other small solutes across cell membranes. Among the different plant AQPs, PIPs (plasma membrane intrinsic proteins), which fall into two phylogenetic groups, PIP1 and PIP2, play key roles in plant water transport processes. PIPs form tetramers in which each monomer acts as a functional channel. The intermolecular interactions that stabilize PIP oligomer complexes and are responsible for the resistance of PIP dimers to denaturating conditions are not well characterized. In the present study, we identified a highly conserved cysteine residue in loop A of PIP1 and PIP2 proteins and demonstrated by mutagenesis that it is involved in the formation of a disulfide bond between two monomers. Although this cysteine seems not to be involved in regulation of trafficking to the plasma membrane, activity, substrate selectivity or oxidative gating of ZmPIP1s (Zm is *Zea mays*), ZmPIP2s and hetero-oligomers, it increases oligomer stability under denaturating conditions. In addition, when PIP1 and PIP2 are co-expressed, the loop A cysteine of ZmPIP1;2, but not that of ZmPIP2;5, is involved in the mercury sensitivity of the channels.

Key words: aquaporin, dimer formation, disulfide bridge, mercury sensitivity, plasma membrane intrinsic protein, trafficking.

INTRODUCTION

As sessile organisms, plants have to tightly control their overall water status. This is partly done through the regulation of water channels, the so-called AQPs (aquaporins), which facilitate water transport across cellular membranes. Plant AQPs belonging to the PIP (plasma membrane intrinsic protein) subfamily play key roles in water and carbon dioxide transport (reviewed in [1–4]). PIPs cluster phylogenetically into two sequence-related groups, PIP1 and PIP2. PIP1s have a longer N-terminal section, a shorter C-terminal section and a shorter extracellular loop A than PIP2s [5,6].

PIP1 and PIP2 isoforms form hetero-oligomers, resulting in altered channel features when expressed in plant cells or *Xenopus laevis* oocytes. PIP2s, but not PIP1s, show high water transport activity when expressed alone in oocytes. However, when PIP1s are co-expressed with PIP2s, a synergistic effect on water channel activity is observed [7–11]. Moreover, when expressed alone in maize cells, PIP1s are retained in the ER (endoplasmic reticulum) and PIP2s are targeted to the plasma membrane, whereas, upon co-expression, PIP1s and PIP2s are co-localized in the plasma membrane as a result of their interaction [12]. In general, PIP1s and PIP2s are simultaneously expressed in the same cells, although certain PIP1 or PIP2 isoforms are specifically expressed in different plant organs or tissues, or at different developmental stages or under different environmental conditions [13,14].

Despite their physiological importance, several specific features of PIPs have not yet been explained at the molecular level. First, PIPs assemble as tetramers in which each monomer acts as a functional channel [15]. Since the first description of PIPs in 1994, many studies have shown that these channels are present as monomers and/or dimers after separation by SDS/PAGE [13,14,16] and that the monomer/dimer ratio depends on the presence of redox-active substances, such as DTT (dithiothreitol), suggesting that PIP1 and PIP2 dimers are covalently linked by disulfide bonds [16–18]. Barone et al. [19] provided experimental evidence that PIP dimers extracted from beetroot are connected by disulfide bonds before their separation by SDS/PAGE, showing that these linkages are not an artefact of sample preparation. Whether the dimers are composed of two identical (homodimers) or different (heterodimers) PIP isoforms is still unknown.

Secondly, the observation that PIP-mediated plant water conductivity is altered by oxidative agents, such as hydroxyl radicals or hydrogen peroxide [20,21], might be explained by oxidative perturbation of the redox state of PIP cysteine residues, leading to changes in the free thiol/disulfide bond ratio or, under conditions of more severe oxidative stress, in the oxidation of the thiol group to a sulfinic, sulfenic or sulfonic acid group. All of these modifications might result in a conformational change, which could change the water permeability of the pore or the protein stability. However, the activity of some AQPs has been shown to be insensitive to oxidation [22].

Thirdly, the activity of some PIPs can be reversely blocked by mercuric chloride [16,23]. Under physiological conditions, mercury (Hg^{2+}) readily interacts with thiol groups of cysteine residues by forming a so-called mercury mercaptide. Mercury is commonly used as an AQP blocker. Mutational studies on mammal AQP1, AQP2, AQP3 and plant TIPs (tonoplast intrinsic

Abbreviations used: AQP, aquaporin; At, *Arabidopsis thaliana*; Av, *Aquilegia vulgaris*; BMS, Black Mexican Sweet; Bv, *Beta vulgaris*; CFP, cyan fluorescent protein; CHX, cycloheximide; DTT, dithiothreitol; ER, endoplasmic reticulum; Ha, *Helianthus annuus*; mCFP, monomeric CFP; NEM, *N*-ethylmaleimide; Ni-NTA, Ni^{2+}-nitrilotriacetate; Nt, *Nicotiana tabacum*; PIP, plasma membrane intrinsic protein; Pp, *Physcomitrella patens*; Pt, *Populus trichocarpa*; So, *Spinacia oleracea*; Tg, *Tulipa gesneriana*; TIP, tonoplast intrinsic protein; WT, wild-type; YFP, yellow fluorescent protein; mYFP, monomeric YFP; Zm, *Zea mays*.

[1] Both of these authors contributed equally to this work.

[2] To whom correspondence should be addressed (email francois.chaumont@uclouvain.be).

proteins) identified certain cysteine residues that are responsible for mercury inhibition [24–27], but no mutational analysis has been performed to identify specific amino acid residues conferring mercury sensitivity in PIPs.

These three experimental observations might potentially be explained by the properties of the PIP cysteine residues.

In the present study, we identified a highly conserved cysteine residue in extracellular loop A of PIP1s and PIP2s that forms a disulfide bridge between PIP monomers and, therefore, plays a role in higher-order oligomer organization. We then tested the biological impact of the formation of disulfide bridges on PIP trafficking, activity, selectivity, stability, interaction and sensitivity to redox compounds, or susceptibility to mercury. Our results showed that the loop A cysteine residue is involved in PIP stability in denaturating conditions and in the sensitivity of PIP1s to mercury. Furthermore our data suggest that the loop A cysteine residue might be involved in the regulation of plasma membrane PIP abundance in plant cells.

MATERIALS AND METHODS

Plasmid construction

The PCR products for the respective PIP isoforms were directionally sub-cloned using a uracil excision-based improved high-throughput USER cloning technique [28] into the USER-compatible *Xenopus* expression vectors pNB1u, pNBRGS-HISu (RGS-His fused to the N-terminal of the protein of interest) and pNB1YFPu [YFP (yellow fluorescent protein) fused to the N-terminal of the protein of interest] [28] or the plant expression vectors pCAMBIA2300 35Su N-term mYFP (monomeric YFP) [29] and pCAMBIA2300 35Su N-term mCFP; the latter plasmid was generated from pCAMBIA2300 35Su [28] and allows the expression of fusion proteins N-terminally tagged with mCFP [monomeric CFP (cyan fluorescent protein)] [12].

Multiple sequence alignment analysis

The program ClustalW [30] was used to perform multiple sequence alignments of full-length or partial PIP protein sequences. The sequences used can be found in the GenBank® data libraries or the DFCI database browser (http://compbio.dfci.harvard.edu/tgi/plant.html) under accession numbers AAY83359 [PpPIP1;1 (Pp is *Physcomitrella patens*)], AAS72892 (PpPIP2;1), BAG68659 [TgPIP1;1 (Tg is *Tulipa gesneriana*)], BAG68661.1 (TgPIP2;1), NP_001104934 [ZmPIP1;2 (Zm is *Zea mays*)], NP_001105024 (ZmPIP2;1), NP_001105616 (ZmPIP2;5), NP_001105027 (ZmPIP2;6), ACT22629 [BvPIP1;1 (Bv is *Beta vulgaris*)], ACT22630 (BvPIP2;2), AAA99274 [SoPIP2;1 (So is *Spinacia oleracea*)], AF440271_1 [NtPIP1;1 (Nt is *Nicotiana tabacum*)], AF440272_1 (NtPIP2;1), PIP11_ARATH [AtPIP1;1 (At is *Arabidopsis thaliana*)], PIP21_ARATH (AtPIP2;1), XP_002315171 [PtPIP1;1 (Pt is *Populus trichocarpa*)], XP_002312952 (PtPIP2;1), TC23220 [AvPIP1 (Av is *Aquilegia vulgaris*)], TC21835 (AvPIP2), TC39835 [HaPIP1 (Ha is *Helianthus annuus*)] and TC39754 (HaPIP2).

Homotetramer models

Homotetramer models of ZmPIP2;5 were built using the Modeller program (version 9v3) [31], which performs comparative modelling by satisfying spatial restraints. We used the X-ray structure of SoPIP2;1 as a template (PDB code 1Z98) [15], with a resolution of 2.1 Å (1 Å = 0.1 nm) and an *R*-factor of 0.183. The sequence identity between ZmPIP2;5 and SoPIP2;1 is approximately 75 %. The pairwise sequence alignment between ZmPIP2;5 and SoPIP2;1 was extracted from PIP plant family multiple alignments. Each pair of chains was defined as a homodimer. On the basis of the sequence alignment, we generated an initial population of 300 models. In these models, the Cys^{75} residues in the extracytosolic loop A of different monomers were very close, but not involved in a disulfide bridge, as the orientation of the Cys^{75} side chains was not favourable for bridge formation. We created a second population of 300 models by imposing a disulfide bridge constraint between Cys^{75} in both homodimers. The Modeller DOPE score was computed for each model. In addition, we used the Zrank [32] and Dfire [33] scoring functions to assess the models. These three scores were then transformed into *z*-scores for normalization purposes. The models were ranked according to the average DOPE, Zrank and Dfire *z*-scores. Finally, model structures were created using PyMOL (http://www.pymol.org).

In vitro RNA synthesis and oocyte transport assays

Ready-to-use capped complementary RNAs encoding tagged or non-tagged ZmPIPs were synthesized *in vitro* as described previously [8]. *Xenopus laevis* oocytes were isolated, defolliculated and injected, and the osmotic water permeability coefficient (P_f) was determined as described previously [8]. Oocytes expressing the YFP-tagged constructs were fixed and sliced as described previously [34]. Fluorescence was visualized by CLSM (confocal laser-scanning microscopy) using a Plan-Neofluar 10×/0.30 objective and quantified with ImageJ software (NIH). The pH inhibition experiment was performed as described previously [7].

Isolation of microsomes from oocytes and maize BMS (Black Mexican Sweet) suspension cells

All steps were carried out at 4 °C. Oocytes were homogenized in 1 ml of homogenization buffer [10 mM KH_2PO_4, 5 mM EDTA and 5 mM EGTA (pH 7.6 with NaOH)] supplemented with 2 μg/ml protease inhibitors (leupeptin, aprotinin, antipain, pepstatin and chymostatin). After centrifugation of the homogenate at 960 ***g*** for 5 min, the supernatant was collected and centrifuged at 2700 ***g*** for 5 min and the resulting supernatant was then centrifuged at 20 800 ***g*** for 50 min and the precipitated microsomes resuspended in suspension buffer [10 mM imidazole and 50 mM KCl (pH 7.5 with HCl)]. The microsomal fraction of BMS cells was prepared as described previously [35].

Cross-linking experiments

Cross-linking reactions were carried out in 150 mM NaCl, 15 mM $Na_3PO_4 \cdot 12H_2O$ and 0.1 mM Tris-bipyridylruthenium (pH 7.5 with HCl). The solution was placed in a tube positioned 2–3 cm from an intense light source (4×36 W) and ammonium persulfate was added at a final concentration of 2.5 mM just before exposure to light for 10 s. The reaction was then immediately stopped by the addition of an equal volume of Laemmli buffer.

Ni-NTA (Ni^{2+}-nitrilotriacetate) co-purification assay

Microsomes of *Xenopus* oocytes co-expressing His_6–ZmPIP2;5 and His_6–ZmPIP1;2 or His_6–ZmPIP2;5(C75A) and His_6–ZmPIP1;2(C85A) were resuspended in 1×PBS buffer. Proteins (300 μg) were solubilized with 1 % (w/v) octyl-β-D-glucopyranoside in a final volume of 400 μl and incubated for 2 h on a rotary wheel at room temperature (21 °C). Unsolubilized material was removed by centrifugation at 53 000 rev./min in a

TLA55-Beckman for 20 min, and the supernatant was added to 100 μl of Ni-NTA agarose matrix (Qiagen) pre-equilibrated with 1×PBS buffer containing 1 % (w/v) octyl-β-D-glucopyranoside and 10 mM imidazole. The mixture was incubated for 2 h on a rotary wheel at room temperature, loaded on to a column, and washed three times with 1 ml of 1×PBS buffer containing 10 mM imidazole and 0.05 % Tween 20. Bound proteins were eluted with 100 μl of 1×PBS buffer containing 250 mM imidazole and 0.05 % Tween 20. Proteins (35 μl/well) were electrophoresed (SDS/PAGE), transferred on to a nitrocellulose membrane, and immunodetected with antibodies raised against ZmPIP1;2 or ZmPIP2;5 [14] using the enhanced bioluminescence method.

Protein analysis

Proteins were solubilized for 15 min at 60 °C in either solubilization buffer [27 mM Tris/HCl, 0.7 % SDS, 3.3 % glycerol and 0.0016 % Bromophenol Blue (pH 6.8)] or solubilization buffer containing the indicated concentration of DTT [if not otherwise stated, 1 % (w/v) DTT was used], and were separated by SDS/PAGE. After protein transfer on to a PVDF membrane, PIPs were immunodetected using antibodies as described in Hachez et al. [14].

Subcellular localization and imaging

Transient expression of mYFP- or mCFP-tagged PIP proteins in maize mesophyll protoplasts was performed as described previously [12]. Confocal images of transfected maize protoplasts or oocyte cells were acquired 1–3 days after transfection using a Zeiss 710 confocal microscope (Carl Zeiss). The YFP was excited with the 514 nm line of an argon multilaser and the emitted YFP fluorescence was detected between 530 and 570 nm. The CFP was excited with the 445 nm line of an argon multilaser and the emitted CFP fluorescence was detected between 462 and 510 nm. In fluorescence decay experiments, two batches of protoplasts were transfected with DNA encoding the WT (wild-type) or mutated ZmPIP2;5 fused to either mYFP or mCFP. The fluorescence signal (F) resulting from the expression of a tagged protein in a cell is defined as $F = k \cdot \Phi \cdot I_0 \cdot c$, where k is a constant, Φ is the quantum efficiency, I_0 is the incident radiant power and c is the molar concentration of the fluorescent dye [36]. Thus, given that Φ and I remain constant, the relationship between the fluorescence intensity and protein concentration is linear. After a 6 h incubation, the two batches were pooled into one well of an eight-well chamber (Lab-Tek, Nalge Nunc International), the fluorescence was checked and 100 μM CHX (cycloheximide) was added to the culture medium. The fluorescence was then monitored over time in both protoplast populations. Image acquisitions were performed every 30 min for a total duration of 16 h using a combination of the time-lapse, tile scan, position and *Z*-stack modules of the Zeiss Zen 2009 software. Fluorescence intensity in the plasma membrane was quantified using ImageJ (NIH) as follows. The *z*-focus corresponding to the equatorial optical cut was extracted from the hyperstack and a thresholding of the pictures was carried out. Then, fluorescence intensity (integrated density) in the plasma membrane was obtained by using the 'analyse particles' function of the software. The following parameters were used: size = 40 − infinity and circularity = 0.00–1.00. The mean value for 7–15 protoplasts expressing WT ZmPIP2;5 or ZmPIP2;5(C75A) were plotted against time in each experiment. Three independent biological replicates were carried out including 50 protoplasts expressing WT ZmPIP2;5 and 47 cells expressing ZmPIP2;5(C75A). Plasma membrane fluorescence was then expressed as a percentage of the initial fluorescence intensity for each population. Slopes corresponding to the rate of fluorescence decay were obtained by linear regression using Microsoft Excel. Means of slopes were calculated for each protoplast population. Student's *t* test was performed to test for significant differences between WT ZmPIP2;5 and ZmPIP2;5(C75A).

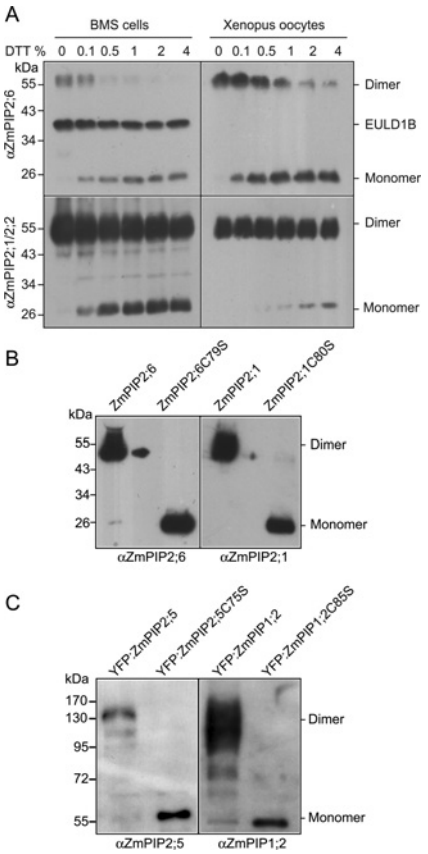

Figure 1 Sensitivity of ZmPIP dimers to different DTT concentrations and involvement of the loop A cysteine residue in the formation of a disulfide bridge between two PIP monomers

(**A**) Microsomes from 14-day-old BMS cultured cells (left-hand panels) or from *Xenopus* oocytes (right-hand panels) expressing ZmPIP2;6 or ZmPIP2;1 were solubilized for 15 min at 60 °C in Laemmli buffer containing increasing concentrations of DTT. The different samples were then loaded on to SDS/PAGE and analysed by Western blotting using affinity-purified antibodies against ZmPIP2;6 (top panels) or ZmPIP2;1/ZmPIP2;2 (bottom panels). The *Z. mays* EULD1B protein, which appears at 38 kDa, is detected by antibodies raised against ZmPIP2;6. (**B** and **C**) Microsomes from oocytes expressing ZmPIP2;6, ZmPIP2;6(C79S), ZmPIP2;1 or ZmPIP2;1(C80S) (**B**), or YFP–ZmPIP2;5, YFP–ZmPIP2;5(C75S), YFP–ZmPIP1;2 or YFP–ZmPIP1;2(C85S) (**C**) were solubilized in Laemmli buffer without DTT and analysed by Western blotting using antibodies raised against the respective ZmPIPs. The positions of monomeric and dimeric PIPs and the molecular mass markers are indicated.

RESULTS

Loop A cysteine residues of PIP1 and PIP2 proteins covalently link monomers and are responsible for the redox-dependent PIP monomer/dimer ratio

After SDS/PAGE separation of microsomal proteins from BMS suspension cells or *Xenopus* oocytes expressing ZmPIP2;1 or ZmPIP2;6, and immunodetection, signals were detected at apparent molecular masses of 26 and 55 kDa corresponding, respectively, to the monomeric and dimeric forms (Figure 1A). The intermediate band at 39 kDa detected using the

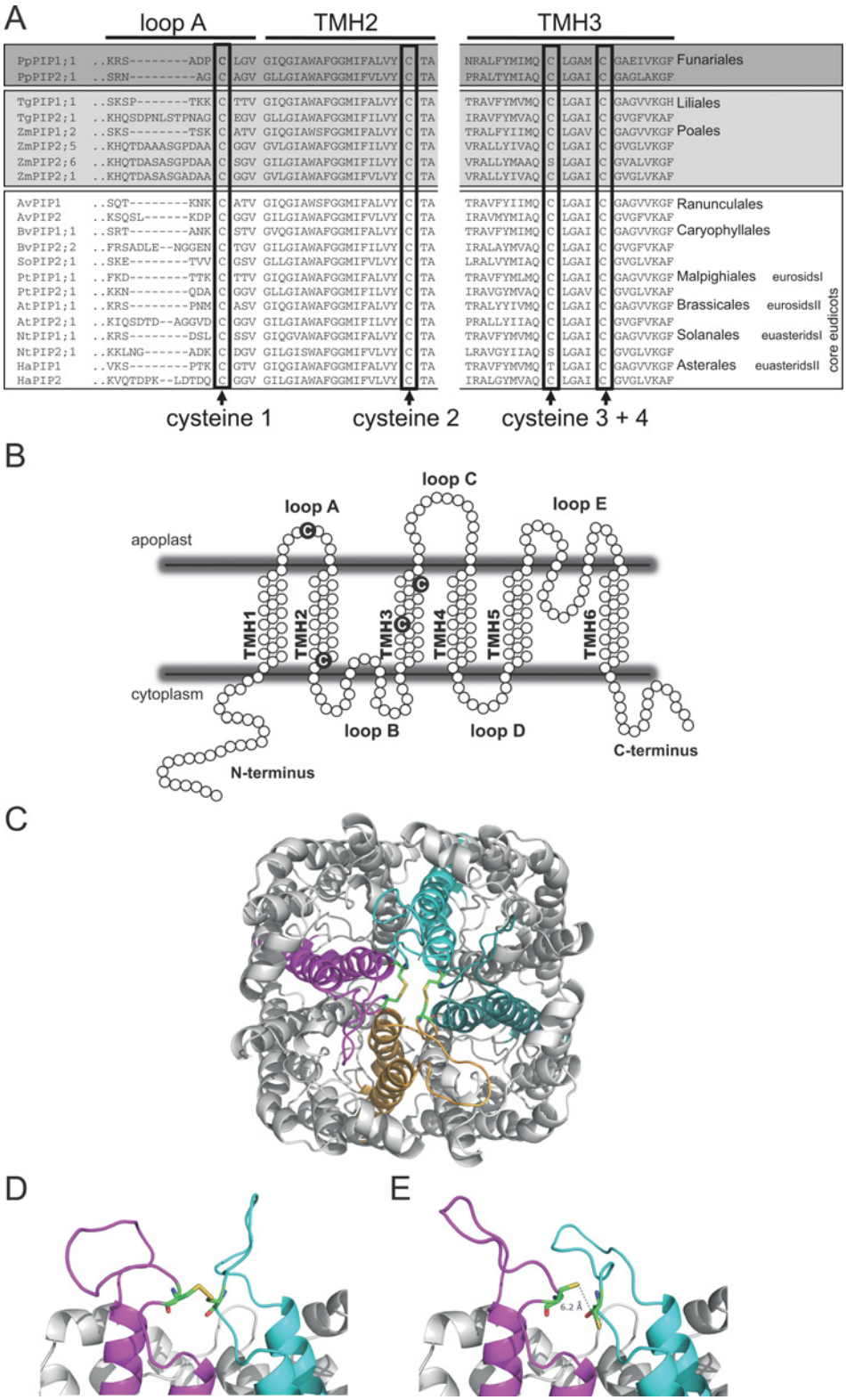

Figure 2 Localization of highly conserved cysteine residues in plant PIP AQPs and a three-dimensional model of ZmPIP2;5 highlighting the disulfide bond between monomers

(**A**) Partial multiple sequence alignment of a variety of plant PIP1 and PIP2 isoforms from non-vascular plants (dark grey box), monocots (light grey box) and eudicots (white box). The plant orders to which the PIPs belong are listed on the right-hand side. Amino acid sequences were compared using the ClustalW program. The four highly conserved cysteine residues are boxed and indicated by arrows. Loop A and the membrane-spanning helices 2 and 3 (TMH2 and TMH3) of crystallized SoPIP2;1 are indicated by a line above the sequence. (**B**) Topological model of a PIP, showing its assembly within the membrane. TMH1 to TMH6 are the six transmembrane helices. The localization of the four highly conserved cysteine residues is indicated. (**C**) Three-dimensional model of the ZmPIP2;5 homotetramer generated as described in the Materials and methods section. The putative disulfide bridges formed between cysteine

anti-ZmPIP2;6 antibodies was not specific and corresponded to EULD1B protein (results not shown) [37]. The PIP dimer/monomer ratio decreased upon the addition of increasing concentrations of the thiol reducing agent DTT to the solubilization buffer, consistent with previous results [16–18]. Interestingly, ZmPIP2;1 and ZmPIP2;6 showed differential sensitivity to DTT, with an intense dimeric band of ZmPIP2;1 still being seen in the presence of 4 % DTT, whereas no, or only a very faint, ZmPIP2;6 band was seen at this DTT concentration (Figure 1A).

A sequence survey of PIP1 and PIP2 isoforms from different plant species (non-vascular, dicot and monocot plants) identified four cysteine residues that are highly conserved among almost all PIP1 and PIP2 isoforms (Figure 2A). According to the SoPIP2;1 X-ray structure [15] and models of the structure of ZmPIP2;5 homotetramers, cysteine 1 is located in extracellular loop A, cysteine 2 is located at the C-terminal end of helix 2 and cysteine residues 3 and 4 are located in helix 3 (Figure 2B). Cysteine residues 2, 3 and 4 are embedded in transmembrane-spanning helices and their thiol groups are oriented in such a way that the formation of a disulfide bond with neighbouring monomers seems very unlikely. However, the cysteine 1 residues in the C-terminus of extracellular loop A of all four monomers are localized remarkably close to each other in the 4-fold axis of the tetramer and seem to cover the putative fifth pore (Figure 2C). Because of their close proximity, these four cysteine residues might chelate metal ions and form hydrogen or disulfide bonds between themselves. To determine whether spatial restraints could allow the formation of disulfide bonds between these cysteine residues, modelling was performed using the program Modeller [31]. The model obtained indicated that a disulfide bond between adjacent PIP monomers could be formed with only a slight change in the conformation of loop A (Figures 2D and 2E). We therefore hypothesized that the loop A cysteine residues might represent the biochemical basis for the observed redox-dependent immunodetection of PIP dimers (Figure 1).

To test this hypothesis, Cys^{80} of ZmPIP2;1, Cys^{75} of ZmPIP2;5, Cys^{79} of ZmPIP2;6 and Cys^{85} of ZmPIP1;2 were mutated into a serine or alanine residue, the proteins were heterologously expressed in oocytes and the PIP isoforms were immunodetected. DTT was not added to the solubilization buffer. In the case of the WT ZmPIP2;1 and ZmPIP2;6 proteins (Figure 1B), and the YFP–ZmPIP1;2 and YFP–ZmPIP2;5 fusion proteins (Figure 1C), intense bands with a molecular mass of approximately 55 kDa or 120 kDa respectively, corresponding to the ZmPIP2;1–ZmPIP2;1, ZmPIP2;6–ZmPIP2;6, YFP–ZmPIP1;2–YFP:ZmPIP1;2 or YFP–ZmPIP2;5–YFP:ZmPIP2;5 dimers were detected, whereas only a single band corresponding to the PIP monomer was detected in the case of the corresponding cysteine-to-serine mutants (Figures 1B and 1C) or the cysteine-to-alanine mutants (results not shown). These results demonstrate that the loop A cysteine residue of ZmPIPs is responsible for the formation of disulfide bridges between two monomers.

Disulfide bonds are formed *in vivo*

To determine whether dimer formation occurred during protein extraction and solubilization, or took place *in vivo*, we incubated BMS suspension cultured cells with different concentrations of NEM (*N*-ethylmaleimide) or iodoacetamide before cell homogenization. These compounds are cell-penetrating thiol-alkylating agents and are used to alkylate free thiol groups to prevent *in vitro* disulfide bond formation. After cell lysis, microsomes were extracted and subjected to Western blot analysis using affinity-purified anti-ZmPIP2;1/ZmPIP2;2 or anti-ZmPIP2;6 antibodies, again without the addition of DTT to the solubilization buffer. As shown in Figure 3, only the dimeric band was detected for both PIP proteins before or after NEM or iodoacetamide treatment, indicating that, in BMS cells, ZmPIP2;1/ZmPIP2;2 and ZmPIP2;6 form dimers linked by disulfide bridges.

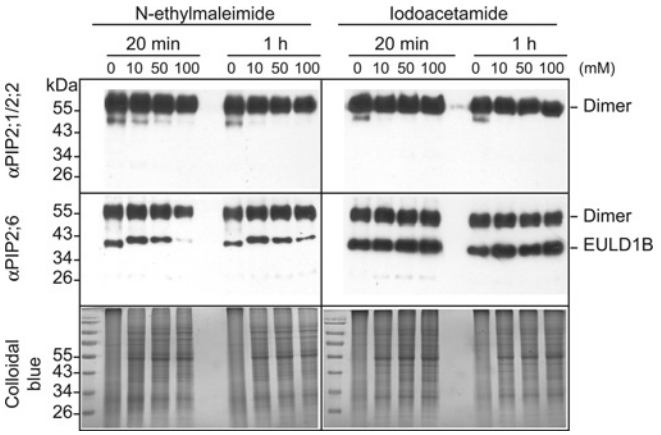

Figure 3 Disulfide bonds between two PIP2 monomers are formed *in vivo*

BMS cells from a 14-day-old cultures were incubated for 20 min or 1 h with 0, 10, 50 or 100 mM NEM (left-hand panels) or iodoacetamide (right-hand panels) to alkylate free thiol groups and to prevent *in vitro* disulfide bond formation. Microsomes were then prepared and subjected to Western blot analysis using affinity-purified anti-ZmPIP2;1 (top panels) or anti-ZmPIP2;6 (middle panels) antibodies. DTT was not included in the Laemmli buffer. The *Z. mays* EULD1B protein, which appears at 38 kDa, is detected by antibodies raised against ZmPIP2;6. A Colloidal Blue-stained gel (bottom panels) was used as a loading control. The position of the molecular mass markers is indicated.

The loop A cysteine residue is not required for PIP trafficking and activity in oocytes

It has been reported that mutation of cysteine residues in mammalian and insect AQPs results in a failure to produce active proteins in oocytes due to retardation in the ER [38,39]. To test whether the cysteine mutants of ZmPIPs were correctly targeted to the oocyte plasma membrane, the localization of YFP–ZmPIP2;5 and YFP–ZmPIP2;5(C75S) was analysed using confocal microscopy. Although no fluorescent signal was detected in water-injected oocytes (results not shown), signals corresponding to the WT YFP–ZmPIP2;5 and mutated forms were detected in the plasma membrane (Figures 4A and 4C), demonstrating that the cysteine mutation did not affect plasma-membrane trafficking. Similar results were obtained with WT and mutated YFP–ZmPIP2;1 or YFP–ZmPIP2;6 isoforms (results not shown). ZmPIP2;5 has been shown to interact with ZmPIP1;2 to increase the amount of the latter in the oocyte membrane [8]. When expressed alone, YFP–ZmPIP1;2 or YFP–ZmPIP1;2(C85S) were barely detectable by

residues in loop A of two adjacent monomers (Cys^{75}) are shown in yellow. The transmembrane helices 1 and 2 and loop A in a given monomer are shown in the same colour and in different colours in different monomers. (**D** and **E**) Zoomed view on Cys^{75} in loop A of two adjacent monomers not forming (**D**) or forming (**E**) a disulfide bond. The pictures are taken from the extracellular side of the tetramer. Sulfur atoms are in yellow. Transmembrane helices 1 and 2 and loop A of the two adjacent monomers are shown in the same colour as in (**C**). The distance between the sulfur atoms is approximately 6.2 Å.

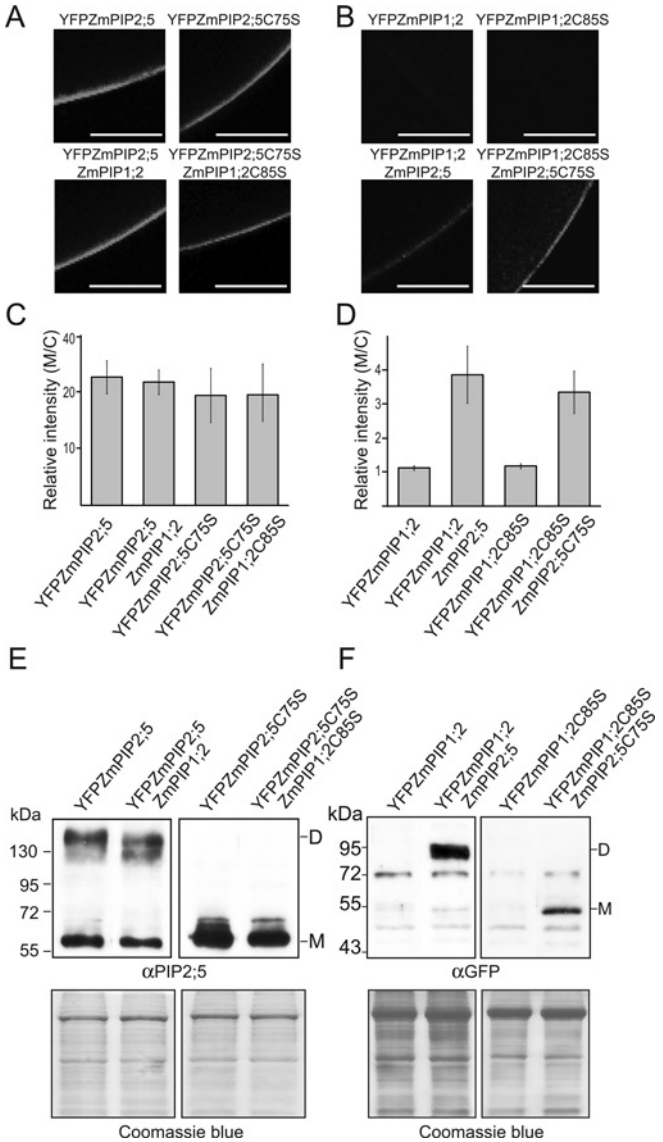

Figure 4 Localization and expression level of WT and mutated mYFP–ZmPIPs (co-) expressed in *Xenopus* oocytes

(**A**) Confocal images of fixed oocytes injected with 4 ng of YFP–ZmPIP2;5 or YFP–ZmPIP2;5(C75S) cRNA or co-injected with 4 ng of YFP–ZmPIP2;5 cRNA and 25 ng of ZmPIP1;2 cRNA, or 4 ng of YFP–ZmPIP2;5(C75S) cRNA and 25 ng of ZmPIP1;2(C85S) cRNA. Acquisitions were done with the same settings. Scale bars = 100 μm. (**B**) Confocal images of fixed oocytes injected with 50 ng of YFP–ZmPIP1;2 or YFP–ZmPIP1;2(C85S) cRNA, or co-injected with 50 ng of YFP–ZmPIP1;2 cRNA and 2 ng of ZmPIP2;5 cRNA, or 50 ng of YFP–ZmPIP1;2(C85S) cRNA and 2 ng of ZmPIP2;5 cRNA. Acquisitions were done with the same settings. Scale bars = 100 μm. (**C** and **D**) Relative YFP fluorescence signal intensity in the plasma membrane (M) compared with the cytoplasm (C) measured with the ImageJ programme. The results are expressed as means from ten oocytes. Error bars are 95 % confidence intervals. (**E** and **F**) Immunodetection of WT and mutated YFP–ZmPIP2;5 (**E**) or YFP–ZmPIP1;2 (**F**) in microsomes (10 μg) from oocytes (co-) expressing the indicated isoforms. The samples were solubilized in Laemmli buffer without DTT. The position of the monomer (M) and the dimer (D) of WT and mutated YFP–ZmPIP2;5 and YFP–ZmPIP1;2 and the molecular mass markers are indicated. The bottom panels show the Coomassie-Brilliant-Blue-stained gels used as loading controls. GFP, green fluorescent protein.

immunodetection or confocal microscopy as previously reported [8] (Figures 4B, 4D and 4F). However, the YFP–ZmPIP1;2 or YFP–ZmPIP1;2(C85S) protein amount found in the microsomal fractions or incorporated into the plasma membrane was much greater when co-expressed with ZmPIP2;5 or ZmPIP2;5(C75S)

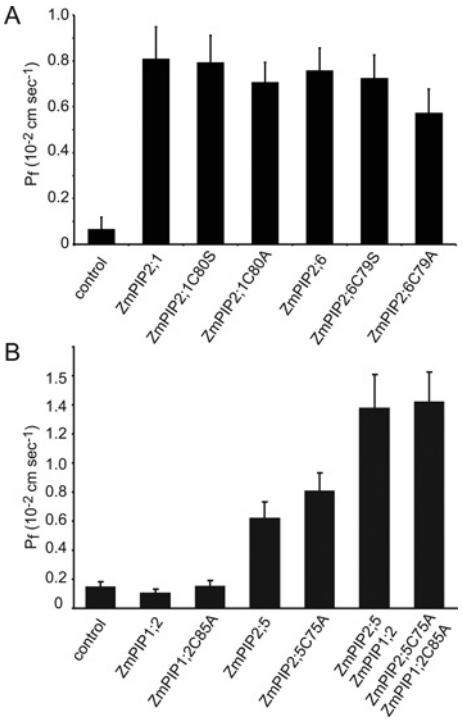

Figure 5 P_f measurements of oocytes expressing WT and mutated ZmPIPs

(**A**) P_f values for oocytes expressing WT ZmPIP2;1 or ZmPIP2;6 or the mutants with a loop A cysteine residue replaced by alanine or serine. (**B**) P_f values for oocytes expressing ZmPIP1;2, ZmPIP2;5, ZmPIP1;2(C85A) or ZmPIP2;5(C75A), or co-expressing ZmPIP1;2 and ZmPIP2;5, or ZmPIP1;2(C85A) and ZmPIP2;5(C75A). In total, 2 ng of ZmPIP2s, or 25 ng of ZmPIP1;2 or ZmPIP1;2(C85A) cRNA was injected. The data are expressed as the mean of measurements from 10 to 19 cells and the error bars represent the 95 % confidence intervals.

(Figures 4B, 4D and 4F). In contrast, the YFP–ZmPIP2;5 or YFP–ZmPIP2;5(C75S) amount did not change upon co-expression with ZmPIP1;2 or ZmPIP1;2(C85S) (Figures 4A, 4C and 4E). These data demonstrate that disulfide bridges between PIP monomers do not affect their trafficking to the plasma membrane or the synergistic effect between ZmPIP2;5 and ZmPIP1;2 leading to a higher amount of the latter in the plasma membrane. We then performed oocyte swelling assays to determine whether the loop A cysteine residue plays a role in the water channel activity of the channels. As shown in Figure 5(A), no significant differences were seen in the membrane osmotic water permeability coefficient (P_f) of oocytes expressing WT ZmPIP2;1, WT ZmPIP2;6, ZmPIP2;1(C80A), ZmPIP2;1(C80S), ZmPIP2;6(C79A) or ZmPIP2;6(C79S). In addition, a similar synergistic effect was seen upon co-expression of either ZmPIP1;2(C85A) and ZmPIP2;5(C75A), or the two WT forms (Figure 5B). These data obtained in oocytes suggest that disulfide bridges between PIP monomers are not important for PIP trafficking, activity and interaction. They also indicate that the higher P_f measured upon co-expression of ZmPIP2;5 and ZmPIP1;2 compared with the P_f value of oocytes expressing ZmPIP2;5 alone is not due to an increased plasma membrane incorporation of ZmPIP2;5, but to a higher amount of ZmPIP1;2.

The loop A cysteine residue of PIP1s and PIP2s is not required for PIP tetramerization

To investigate whether the disulfide bridges were required for tetramerization, a cross-linking experiment was performed on microsomes from oocytes expressing ZmPIP2;6 (able to form

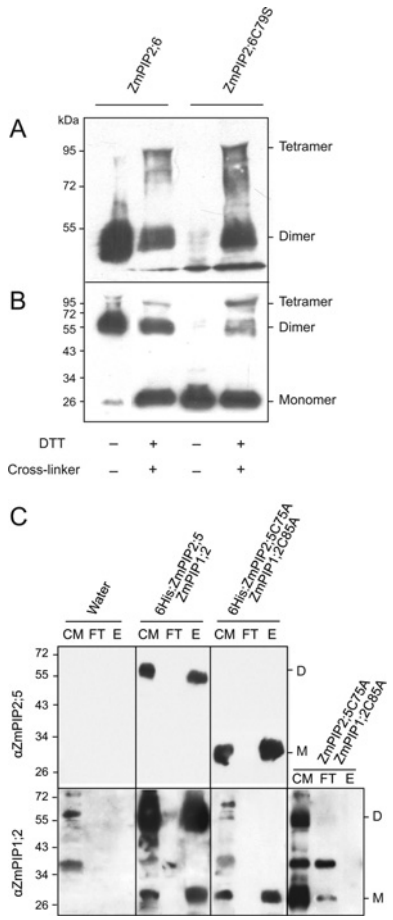

Figure 6 Tetramerization and interaction of ZmPIPs occur independently of their ability to form a disulfide bridge between PIP monomers

(**A** and **B**) Non-solubilized microsomes extracted from oocytes expressing ZmPIP2;6 or ZmPIP2;6(C79S) were treated with the cross-linker Tris-bipyridylruthenium (0.1 mM, 10 s), and then Laemmli buffer containing DTT was added to stop the reaction. The treated and non-treated samples were then loaded on 8 % (**A**) or 12 % (**B**) acrylamide gels and analysed by Western blotting using anti-ZmPIP2;6 antibodies. The monomeric, dimeric and tetrameric forms are indicated. The position of the molecular mass markers is indicated. (**C**) Microsomal fractions from oocytes co-expressing His_6–ZmPIP2;5 and ZmPIP1;2, His_6–ZmPIP2;5(C75A) and ZmPIP1;2(C85A), or ZmPIP2;5(C75A) and ZmPIP1;2(C85A) were solubilized with n-octyl-β-D-glucopyranoside. After ultracentrifugation, membrane protein extracts were loaded on to Ni-NTA columns. Microsomal (CM), flow-through (FT) and eluted (E) fractions were analysed by immunodetection using antibodies raised against ZmPIP2;5 and ZmPIP1;2. The monomeric (M) and dimeric (D) forms are indicated. Oocytes injected with water were used as a control. The samples were solubilized in Laemmli buffer without DTT. Note that ZmPIP1;2(C85A) proteins were co-purified with His_6–ZmPIP2;5(C75A) as monomers and that non-specific bands at approximately 38, 58 and 80 kDa were detected by the anti-ZmPIP1;2 antibodies in oocyte microsomes. The position of the molecular mass markers is indicated.

disulfide-linked dimers) or ZmPIP2;6(C79S) (no dimer formation in denaturating conditions) (Figure 1). Tris-bipyridylruthenium, a compound which allows the formation of a covalent link between a tyrosine residue and a tyrosine, lysine or cysteine residue was used as a photo-inducible cross-linker [40]. This compound considerably reduces the time for the cross-linking reaction and, therefore, possible artefact formation. After treatment, microsomal proteins were subjected to Western blot analysis using anti-ZmPIP2;6 antibodies (Figures 6A and 6B). A signal at approximately 100 kDa, probably corresponding to the tetrameric form, was observed after cross-linking in microsomes containing either ZmPIP2;6 or ZmPIP2;6(C79S), indicating that disulfide bridges linking PIP loops A are not required for tetramerization.

As shown by Fetter et al. [8], heterotetramer formation might explain the observed synergistic effect on the water channel activity. To determine whether the loop A cysteine residues of PIP1s and PIP2s substantially affect this hetero-oligomerization process, we performed a chromatography co-purification approach [8] using microsomes from oocytes co-expressing WT or mutated His_6–ZmPIP2;5 and His_6–ZmPIP1;2. After solubilization of His_6–ZmPIP2;5 or His_6–ZmPIP2;5(C75A) using octyl-β-D-glucopyranoside and purification on a Ni-NTA column, the presence of ZmPIP1;2 or ZmPIP1;2(C85A) in the eluted fractions was checked by immunodetection (Figure 6C). As expected from previous reports [8,41], ZmPIP1;2 was present in the eluted fractions coming from oocytes co-expressing His_6–ZmPIP2;5 and ZmPIP1;2. Similar results were obtained after performing the same procedure with microsomes from oocytes co-expressing ZmPIP1;2(C85A) and His_6–ZmPIP2;5(C75A). In this case, both proteins appeared as monomers instead of dimers. When microsomes from oocytes co-expressing non-tagged ZmPIPs were loaded on to a column, ZmPIP1;2(C85A) could not be detected in the eluted fraction (Figure 6C). These data demonstrate that the co-purification does not result from a non-specific binding of ZmPIP1;2(C85A) to the Ni-NTA column, but that mutated ZmPIP1;2 and ZmPIP2;5 are still able to physically interact. Although the formation of disulfide bridges is importantly affecting the dimer stability, it is not required for a functional heterotetramer formation.

The loop A cysteine residue of ZmPIP2 proteins is not sensitive to redox-reactive treatment

Oxidative gating of AQPs by ROS (reactive oxygen species) has been suggested in several studies performed on Chara cells, and maize roots and leaves [20,21,42], but the precise mechanism was not investigated. We tested whether the loop A cysteine residue involved in disulfide bond formation between PIP monomers had an effect on oxidative or reductive treatments that might affect PIP gating. This hypothesis was investigated by measuring the P_f value of oocytes expressing WT ZmPIP2;5 or ZmPIP2;5(C75S) after treatment with oxidants (H_2O_2 or t-butylhydroperoxide) or reductants (2-mercaptoethanol or DTT). No significant differences were observed in the P_f values for non-treated or oxidant-treated (Figure 7A) or reductant-treated (Figure 7B) oocytes, indicating that the disulfide bonds, as well as other potential modifications of the cysteine thiol group, do not affect the activity of ZmPIP2;5. Similar results were obtained using ZmPIP2;6 (results not shown).

The loop A cysteine residue of ZmPIP1;2, but not that of ZmPIP2;5, is involved in mercury sensitivity

ZmPIP2;5 is inhibited by mercury chloride [23]. To investigate whether the loop A cysteine residue of ZmPIP2;5 accounts for the mercury sensitivity, ZmPIP2;5 and ZmPIP2;5(C75S) were expressed alone or together with ZmPIP1;2 or ZmPIP1;2(C85S) in oocytes and the effect of $HgCl_2$ on the P_f value was examined. In this experiment, we injected twice the ZmPIP2;5 cRNA amount compared with Figure 5(B) to obtain a higher P_f value and to easily detect the effect of mercury. As shown in Figure 7(C), $HgCl_2$ treatment resulted in a similar inhibition of the P_f value of oocytes expressing ZmPIP2;5 or ZmPIP2;5(C75S), demonstrating that Cys^{75} is not responsible for the mercury sensitivity. Although the P_f value of cells co-expressing ZmPIP1;2 and ZmPIP2;5 was strongly inhibited by $HgCl_2$, the P_f value of cells co-expressing ZmPIP1;2(C85S) and ZmPIP2;5(C75S) was insensitive to $HgCl_2$. A similar lack of inhibition was seen in oocytes co-expressing

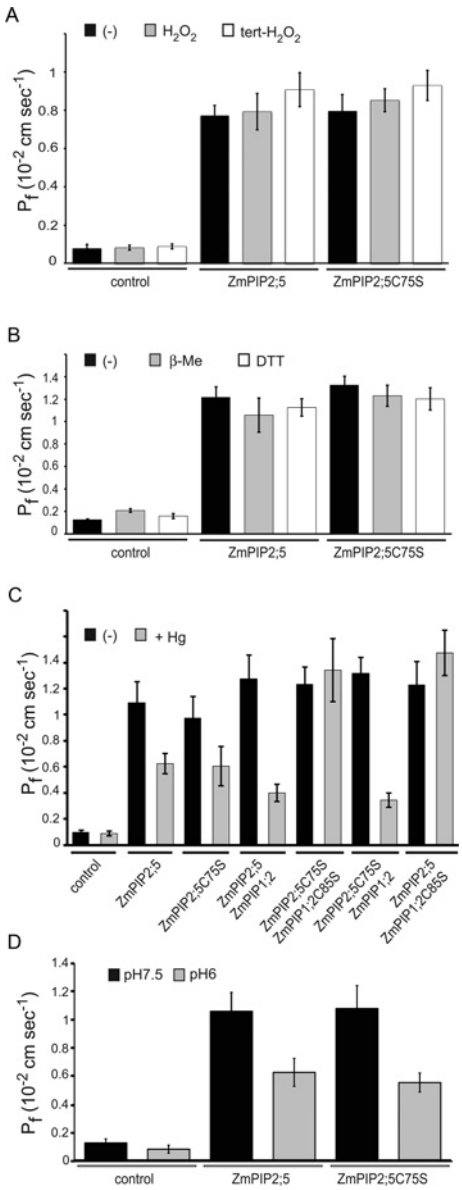

Figure 7 Effects of reducing or oxidizing compounds, pH or mercury, on the P_f value of oocytes expressing WT and mutated ZmPIPs

The P_f value of oocytes injected with water (control) or 4 ng of ZmPIP2;5 or ZmPIP2;5(C75S) cRNA or co-injected with 4 ng of ZmPIP2;5 or ZmPIP2;5(C75S) cRNA, and 25 ng of ZmPIP1;2 or ZmPIP1;2(C85S) cRNA in the absence (black bars) or presence of 2 mM H_2O_2 (**A**, grey bars), 2 mM t-butylhydroperoxide (**A**, white bars), 5 mM 2-mercaptoethanol (**B**, grey bars), 4 % DTT (**B**, white bars), 1 mM $HgCl_2$ (**C**, grey bars), at pH 6 (**D**, grey bars) or pH 7.5 (**D**, black bars). For each treatment, oocytes were incubated with the redox compound or at the respective pH for 15–20 min before the water swelling assay. The data are expressed as the mean of measurements from 7 to 19 cells and the error bars represent the 95 % confidence intervals.

ZmPIP2;5 and ZmPIP1;2(C85S). In contrast, $HgCl_2$ inhibited the P_f value of oocytes co-expressing ZmPIP2;5(C75S) and ZmPIP1;2. These results suggest that ZmPIP1;2 Cys^{85} is involved in the mercury sensitivity of PIP hetero-oligomers, but ZmPIP2;5 Cys^{75} is not.

The loop A cysteine residue of ZmPIP2;5 does not play a role in its pH inhibition

A conserved cytoplasmic histidine residue in loop D was shown to be responsible for the pH-dependence of PIP gating [43]. An additional pH effect due to extracellular amino acid residues might be possible. As cysteine residues can be protonated, we tested whether the loop A cysteine residue had an impact on the pH regulation of the P_f value. This hypothesis was investigated by measuring the P_f value of oocytes expressing WT ZmPIP2;5 or ZmPIP2;5(C75S) after their incubation in a buffer solution with non-inhibitory (pH 7.5) and inhibitory (pH 6) pH values [7]. Oocytes expressing the mutated or the WT ZmPIP2;5 showed a similar inhibitory response at pH 6 (Figure 7D), indicating that the pH does not affect the activity of ZmPIP2;5 via the cysteine thiol group.

The loop A cysteine residue of PIP1s and PIP2s is not required for PIP localization and co-trafficking to the plant plasma membrane

We previously showed that the physical interaction between fluorescent-tagged ZmPIP1s and ZmPIP2s is required for an efficient re-localization of ZmPIP1s from the ER to the plasma membrane in plant cells [12]. To test whether the disulfide bridge between PIP monomers was necessary for this process, we studied the localization of mCFP–ZmPIP1;2(C85S) and mYFP–ZmPIP2;5(C75S) expressed singly or together in maize mesophyll protoplasts using confocal microscopy. Protoplasts transiently expressing mYFP–ZmPIP2;5 (Figure 8A) or mYFP–ZmPIP2;5(C75S) (Figure 8B) showed similar sharp fluorescent signals in the plasma membrane, whereas mYFP–ZmPIP1;2 (Figure 8C) and mYFP–ZmPIP1;2(C85S) (Figure 8D) were detected in the ER. Co-expression of mYFP–ZmPIP2;5(C75S) and mCFP–ZmPIP1;2(C85S) still resulted in the re-localization of mCFP–ZmPIP1;2(C85S) to the plasma membrane and a perfect co-localization with mYFP–ZmPIP2;5(C75S) therein (Figures 8E, 8F, 8I, 8J, 8M and 8N). When internalization of PIPs from the plasma membrane to internal membrane structures was induced by salt stress, both PIP isoforms were still perfectly co-localized (Figures 8G, 8H, 8K, 8L, 8O and 8P). These results show that the formation of covalently linked dimers of PIP1s or PIP2s is not essential for their localization or trafficking to and from the plasma membrane, and that a disulfide bond between PIP1s and PIP2s is not responsible for the co-trafficking of the two isoforms.

Do loop A cysteine residues affect the PIP stability in plant cells?

To investigate whether the disulfide bridges are involved in the stability of PIPs in plant cells, we monitored the stability of WT and mutated ZmPIP2;5 in the plasma membrane of maize protoplasts. We first determined the time course of expression of mYFP–ZmPIP2;5 in protoplasts by monitoring the fluorescent signal from 30 min to 16 h after poly(ethylene glycol)-mediated transfection; the latter time point corresponds to the incubation time routinely used in protoplast expression-based assays [12,44]. As shown in Supplementary Figure S1 (at http://www.BiochemJ.org/bj/445/bj4450101add.htm), mYFP–ZmPIP2;5 fluorescence was clearly detectable in the plasma membrane 6 h after transfection. The fate of pre-formed mYFP–ZmPIP2;5 was then studied in cells treated with 100 μM CHX 6 h after transfection to prevent the synthesis and plasma membrane delivery of new protein. In this system, a decrease in the fluorescent signal was already detectable 1.5 h after CHX addition (results not shown). mCFP–ZmPIP2;5(C75A) or mYFP–ZmPIP2;5 was then expressed singly in protoplasts, the cells were mixed and the fluorescence intensity of each protein was simultaneously monitored in a time-lapse experiment, using acquisition settings optimized to obtain a similar level of fluorescence for both of the tagged proteins at the first acquisition

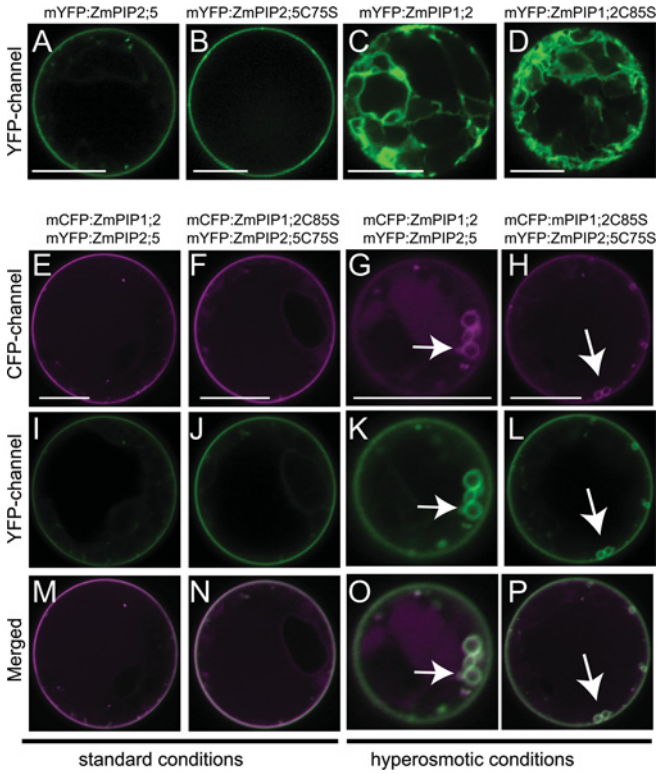

Figure 8 Subcellular localization of WT and mutated mCFP–ZmPIP1;2 and mYFP–ZmPIP2;5 expressed in maize protoplasts

(**A**–**D**) Mesophyll protoplasts transiently expressing mYFP–ZmPIP2;5 (**A**), mYFP–ZmPIP2;5(C75S) (**B**), mYFP–ZmPIP1;2 (**C**) or mYFP–ZmPIP1;2(C85S) (**D**). WT and mutated ZmPIP isoforms show a similar subcellular localization in the plasma membrane (**A** and **B**) or the ER (**C** and **D**). (**E**–**P**) Mesophyll protoplasts transiently co-expressing mYFP–ZmPIP2;5 + mCFP–ZmPIP1;2 (**E**, **I**, **M**, **G**, **K** and **O**) or mYFP–ZmPIP2;5(C75S) + mCFP–ZmPIP1;2(C85S) (**F**, **J**, **N**, **H**, **L** and **P**) under standard conditions (**E**, **F**, **I**, **J**, **M** and **N**) or after hypertonic treatment (500 mM NaCl) (**G**, **H**, **K**, **L**, **O** and **P**). Top row, mCFP fluorescence; middle row, mYFP fluorescence; bottom row, merged images. The arrows indicated internalized PIP-labelled plasma-membrane-derived vesicles. Scale bars = 10 μm.

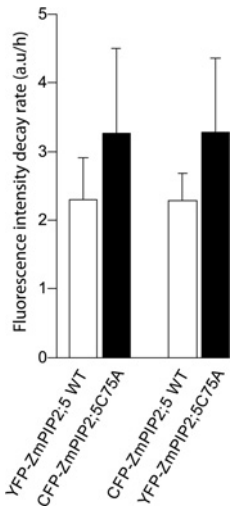

Figure 9 Plasma membrane stability of ZmPIP2;5(C75A) compared with WT ZmPIP2;5

Maize mesophyll protoplasts expressing mYFP–ZmPIP2;5, mCFP–ZmPIP2;5(C75A), mCFP–ZmPIP2;5 or mYFP–ZmPIP2;5(C75A) were monitored by time-lapse video microscopy using a confocal microscope. At 6 h after transfection, a signal was detected in the plasma membrane for both populations and the translation inhibitor CHX (100 μM) was added to the culture medium. The protoplast fluorescence was then monitored every 30 min for 16 h. Open and filled bars represent the mean of fluorescence decay slopes calculated on three independent experiments including 50 and 47 protoplasts expressing WT ZmPIP2;5 and ZmPIP2;5(C75A) respectively. Error bars represent the confidence interval at 95 %. Student's *t* test showed no statistically significant difference. a.u., absorbance units.

point. The level of fluorescence in the plasma membrane at each time point and the resulting decay slopes were determined by picture analysis (for further details see the Materials and methods section). The fluorescence decay rate (i.e. the decrease of mYFP–ZmPIP abundance in the plasma membrane) was slightly higher in protoplasts expressing mYFP–ZmPIP2;5(C75A) than in cells expressing WT mYFP–ZmPIP2;5 (Figure 9). However, this difference was not statistically significant. Similar results were obtained when the two fluorophores were swapped (Figure 9).

DISCUSSION

The very first paper dealing with plant PIP AQPs in 1994 reported that PIP proteins can be detected by SDS/PAGE as monomers and dimers, and that their ratio depends on the redox conditions [16]. The authors formulated the hypothesis that "PIP proteins are cross-linked by at least one disulfide bond" and that an extracellularly located cysteine residue might be a potential site for the formation of such a bond. Since then, the biochemical reason for the occurrence of PIP dimers in SDS/PAGE remained undetermined.

Using mutational analysis, we identified a highly conserved extracellular cysteine residue in loop A of both PIP1s and PIP2s that is responsible for the formation of a disulfide bond between monomers and the detection of dimers by SDS/PAGE and Western blotting. We demonstrated that, under denaturing conditions, the stability of PIP dimers was increased by this covalent bonding. Furthermore, we showed that this covalent linkage of ZmPIP monomers occurred in plant cells and was not due to sample preparation, confirming the observations of Barone et al. [19]. Although the loop A cysteine residue was important for the formation of PIP dimers, it was not required for homo- or hetero-tetramerization. This was to be expected, as many plant, microbial or mammalian AQPs assemble as tetramers, even though they do not possess a similar cysteine residue. Nevertheless, the evolutionary conservation of this loop A cysteine residue suggests a specific role. Accurate folding in the ER and consequently the correct localization of a large number of proteins, including AQPs [38,39], are known to depend on cysteine residues. In this regard, the possibility of a covalent interaction between PIP monomers is of special interest, as a physical interaction between PIP1 and PIP2 isoforms regulate their trafficking in plant cells [12] and in oocytes [8]. However, PIPs with a mutated loop A cysteine residue did not show altered trafficking in maize protoplasts and oocytes in our test conditions. Furthermore, functional assays in oocytes showed that the absence of covalent-linked PIP dimers did not affect the water channel activity of PIPs when expressed alone (PIP2s) or co-expressed (PIP1–PIP2). Co-purification assays confirmed that the interaction between PIP1 and PIP2 also occurred in the absence of covalently linked PIP dimers. Therefore formation of homo- or hetero-tetramers appeared to not depend on the presence of disulfide bridges. No change in the P_f value was detected after treatment with reducing or oxidative agents, demonstrating that this cysteine residue is not responsible for the suggested redox sensitivity of PIPs [17,20,21]. This insensitivity to oxidation has also been observed for AtPIP2;1 and AtTIP1;1 [22]. In contrast, Ampilogova et al. [17] clearly demonstrated that a change in

the ratio of thiol and disulfide bonds in plant plasma membrane proteins correlates with a change in water permeability. These conflicting observations might be explained by the fact that the AQP-mediated decrease in membrane permeability is not due to direct oxidation of the channel, but rather to a secondary effect, e.g. a re-localization of AQPs to internal structures [22]. Such a regulating mechanism may be absent in oocytes.

The mercury inhibition data are interesting in terms of the potential functional and conformational interaction between PIP1s and PIP2s in hetero-oligomer complexes. Cys^{75} of ZmPIP2;5 was found not to be responsible for the known mercury sensitivity of ZmPIP2;5 [23], as WT ZmPIP2;5 and the ZmPIP2;5(C75S) mutant were inhibited to a similar extent by $HgCl_2$. In contrast, the P_f value of oocytes co-expressing ZmPIP1;2(C85S) and WT ZmPIP2;5 or ZmPIP2;5(C75S) was not decreased in response to $HgCl_2$ treatment, indicating that, when ZmPIP2;5 was co-expressed with ZmPIP1;2(C85S), ZmPIP2;5 became mercury-insensitive. This observation strongly suggests that the loop A cysteine residue of ZmPIP1;2 is responsible for the mercury sensitivity of the hetero-oligomers. Furthermore, these results may indicate that the conformational arrangement of PIP2 monomers in PIP1–PIP2 hetero-oligomers is different from that in PIP2 homo-oligomers, as otherwise a mercury inhibition of ZmPIP2;5 should be observed when being co-expressed with ZmPIP1;2(C85S). As no structural data are available for PIP1–PIP2 hetero-oligomers, and since loop A is one of the most divergent regions between PIP1s and PIP2s, it is difficult at this stage to speculate about the mechanistic basis for this difference. Interestingly, mercury itself has been shown to induce conformational changes in extracellular loops of PIP2s from *B. vulgaris* [45].

A previous study revealed a differential behaviour of co-expressed PIP1–PIP2 proteins and PIP2s expressed alone [7]. Co-expression of BvPIP1 and BvPIP2 proteins from *B. vulgaris* not only synergistically increases the oocyte P_f, but also markedly increases the inhibitory effect of cytosolic acidification on PIP activity. Furthermore, the tetramer composition (PIP1/PIP2 ratio) modifies the function of tobacco PIPs transporting either carbon dioxide or water [46]. Taking all of these data together, it appears that the monomer composition of PIP tetramers regulates their function and regulation, possibly through a conformational rearrangement of the extracellular loops.

With regard to the mercury sensitivity of single PIPs, the amino acid residue responsible has still to be identified. Although all of the PIP1 and PIP2 isoforms possess the same four cysteine residues, some are mercury-sensitive [23], whereas others, such as AtPIP2;1 and AtPIP2;3, are not [16,47,48], indicating that the presence of cysteine residues alone is not sufficient to cause mercury sensitivity and that other features must be taken into account. The comparison of the stability of WT and mutated ZmPIP2;5 in the plasma membrane of transfected maize cells indicated a slight faster decay of ZmPIP2;5(C75A) independent of the fused fluorescent tag; however, the difference was not significant. It is possible that PIP tetramer stabilization through the association of covalently linked dimers could be important under different physiological or stress conditions that remain to be determined. Such a stabilization role has, for instance, been attributed to the disulfide bonds linking the *Arabidopsis* ethylene receptor ETR1; as observed for PIPs, mutation of the involved cysteine residues did not affect protein function [49]. Disulfide bonds are known to be important for the physical and chemical stability of proteins [50]. Factors that influence the physical and chemical stability of a protein can be divided into two categories: (i) intrinsic factors due to the inherent physicochemical properties of the protein (e.g. primary, secondary, tertiary and quaternary structures) and (ii) extrinsic factors due to the environment of the protein, such as pH, temperature, proteases, buffer or ionic strength [50]. A closer investigation of the role of the disulfide bond in PIP stability under different conditions is required.

Finally, we cannot exclude the possibility that the formation of disulfide bonds between PIP monomers plays an important role in tetramer composition and the proper regulation of transmembrane transport processes. All different PIP monomers could potentially interact with each other within a tetramer ([12,41] and D. Cavez and F. Chaumont, unpublished work). Moreover, several studies have shown modified PIP traits upon the co-expression of different PIP isoforms [7–11,46]. However, for efficient regulation and fine-tuning of transmembrane water or solute transport, it seems obvious that AQP tetramers should not be assembled by a random arrangement of various isoforms. The covalent-bonded dimerization of PIPs in the ER might ensure that only tetramers of specific compositions are formed and leave the ER. Preliminary results obtained in our laboratory suggest that disulfide bridges favour the formation of homodimers (D. Cavez, M.C. Berny, G.P. Bienert, A. Besserer and F. Chaumont, unpublished work). This limitation in tetramer composition would allow a higher order of quaternary structure and therefore a more specific regulation of PIP function. In addition, a recent biochemical study investigated the folding and/or unfolding mechanisms of the tetrameric aquaglyceroporin GlpF and showed that this process occurs via a stable dimeric intermediate [51]. On the basis of their experimental data, the authors suggest that the formation of the quaternary structure of GlpF proceeds from a monomer to a dimer and two dimers then form a tetramer. Our results not only support this hypothesis, but furthermore identify the loop A cysteine residue as one key residue playing a role in the stabilization of the dimeric form of plant PIP AQPs, at least under certain conditions.

AUTHOR CONTRIBUTION

Gerd Bienert, Damien Cavez and Arnaud Besserer designed and carried out the experimental work, analysed data and wrote the paper. Marie Berny, Dimitri Gilis and Marianne Rooman carried out the models and wrote the corresponding part of the paper. François Chaumont designed the experiments, analysed the data and wrote the paper.

FUNDING

This work was supported by the Belgian National Fund for Scientific Research (FNRS), the Interuniversity Attraction Poles Programme-Belgian Science Policy, and the "Communauté française de Belgique-Actions de Recherches Concertées". G.P.B. was supported by an individual Marie Curie European fellowship. D.C. and M.B. were Research Fellows at the "Fonds pour la Formation à la Recherche dans l'Industrie et dans l'Agriculture". A.B. was a Postdoctoral Research Fellow at the FNRS.

REFERENCES

1 Chaumont, F., Moshelion, M. and Daniels, M. J. (2005) Regulation of plant aquaporin activity. Biol. Cell **97**, 749–764

2 Evans, J. R., Kaldenhoff, R., Genty, B. and Terashima, I. (2009) Resistances along the CO_2 diffusion pathway inside leaves. J. Exp. Bot. **60**, 2235–2248

3 Gomes, D., Agasse, A., Thiebaud, P., Delrot, S., Geros, H. and Chaumont, F. (2009) Aquaporins are multifunctional water and solute transporters highly divergent in living organisms. Biochim. Biophys. Acta **1788**, 1213–1228

4 Maurel, C., Verdoucq, L., Luu, D. T. and Santoni, V. (2008) Plant aquaporins: membrane channels with multiple integrated functions. Annu. Rev. Plant Biol. **59**, 595–624

5 Chaumont, F., Barrieu, F., Wojcik, E., Chrispeels, M. J. and Jung, R. (2001) Aquaporins constitute a large and highly divergent protein family in maize. Plant Physiol. **125**, 1206–1215

6 Johanson, U., Karlsson, M., Johansson, I., Gustavsson, S., Sjovall, S., Fraysse, L., Weig, A. R. and Kjellbom, P. (2001) The complete set of genes encoding major intrinsic proteins in *Arabidopsis* provides a framework for a new nomenclature for major intrinsic proteins in plants. Plant Physiol. **126**, 1358–1369

7 Bellati, J., Alleva, K., Soto, G., Vitali, V., Jozefkowicz, C. and Amodeo, G. (2010) Intracellular pH sensing is altered by plasma membrane PIP aquaporin co-expression. Plant Mol. Biol. **74**, 105–118

8 Fetter, K., Van Wilder, V., Moshelion, M. and Chaumont, F. (2004) Interactions between plasma membrane aquaporins modulate their water channel activity. Plant Cell **16**, 215–228

9 Temmei, Y., Uchida, S., Hoshino, D., Kanzawa, N., Kuwahara, M., Sasaki, S. and Tsuchiya, T. (2005) Water channel activities of *Mimosa pudica* plasma membrane intrinsic proteins are regulated by direct interaction and phosphorylation. FEBS Lett. **579**, 4417–4422

10 Vandeleur, R. K., Mayo, G., Shelden, M. C., Gilliham, M., Kaiser, B. N. and Tyerman, S. D. (2009) The role of plasma membrane intrinsic protein aquaporins in water transport through roots: diurnal and drought stress responses reveal different strategies between isohydric and anisohydric cultivars of grapevine. Plant Physiol. **149**, 445–460

11 Mahdieh, M. and Mostajeran, A. (2009) Abscisic acid regulates root hydraulic conductance via aquaporin expression modulation in *Nicotiana tabacum*. J. Plant Physiol. **166**, 1993–2003

12 Zelazny, E., Borst, J. W., Muylaert, M., Batoko, H., Hemminga, M. A. and Chaumont, F. (2007) FRET imaging in living maize cells reveals that plasma membrane aquaporins interact to regulate their subcellular localization. Proc. Natl. Acad. Sci. U.S.A. **104**, 12359–12364

13 Hachez, C., Heinen, R. B., Draye, X. and Chaumont, F. (2008) The expression pattern of plasma membrane aquaporins in maize leaf highlights their role in hydraulic regulation. Plant Mol. Biol. **68**, 337–353

14 Hachez, C., Moshelion, M., Zelazny, E., Cavez, D. and Chaumont, F. (2006) Localization and quantification of plasma membrane aquaporin expression in maize primary root: a clue to understanding their role as cellular plumbers. Plant Mol. Biol. **62**, 305–323

15 Tornroth-Horsefield, S., Wang, Y., Hedfalk, K., Johanson, U., Karlsson, M., Tajkhorshid, E., Neutze, R. and Kjellbom, P. (2006) Structural mechanism of plant aquaporin gating. Nature **439**, 688–694

16 Kammerloher, W., Fischer, U., Piechottka, G. P. and Schaffner, A. R. (1994) Water channels in the plant plasma membrane cloned by immunoselection from a mammalian expression system. Plant J. **6**, 187–199

17 Ampilogova, Y. N., Zhestkova, I. M. and Trofimova, M. S. (2006) Redox modulation of osmotic water permeability in plasma membranes isolated from roots and shoots of pea seedlings. Russ. J. Plant Physiol. **53**, 622–628

18 Qi, X., Tai, C. Y. and Wasserman, B. P. (1995) Plasma membrane intrinsic proteins of *Beta vulgaris* L. Plant Physiol. **108**, 387–392

19 Barone, L. M., Mu, H. H., Shih, C. J., Kashlan, K. B. and Wasserman, B. P. (1998) Distinct biochemical and topological properties of the 31- and 27-kilodalton plasma membrane intrinsic protein subgroups from red beet. Plant Physiol. **118**, 315–322

20 Kim, Y. X. and Steudle, E. (2008) Gating of aquaporins by light and reactive oxygen species in leaf parenchyma cells of the midrib of *Zea mays*. J. Exp. Bot. **60**, 547–556

21 Ye, Q. and Steudle, E. (2006) Oxidative gating of water channels (aquaporins) in corn roots. Plant, Cell Environ. **29**, 459–470

22 Boursiac, Y., Boudet, J., Postaire, O., Luu, D. T., Tournaire-Roux, C. and Maurel, C. (2008) Stimulus-induced downregulation of root water transport involves reactive oxygen species-activated cell signalling and plasma membrane intrinsic protein internalization. Plant J. **56**, 207–218

23 Chaumont, F., Barrieu, F., Jung, R. and Chrispeels, M. J. (2000) Plasma membrane intrinsic proteins from maize cluster in two sequence subgroups with differential aquaporin activity. Plant Physiol. **122**, 1025–1034

24 Daniels, M. J., Chaumont, F., Mirkov, T. E. and Chrispeels, M. J. (1996) Characterization of a new vacuolar membrane aquaporin sensitive to mercury at a unique site. Plant Cell **8**, 587–599

25 Kuwahara, M., Gu, Y., Ishibashi, K., Marumo, F. and Sasaki, S. (1997) Mercury-sensitive residues and pore site in AQP3 water channel. Biochemistry **36**, 13973–13978

26 Preston, G. M., Jung, J. S., Guggino, W. B. and Agre, P. (1993) The mercury-sensitive residue at cysteine 189 in the CHIP28 water channel. J. Biol. Chem. **268**, 17–20

27 Bai, L. Q., Fushimi, K., Sasaki, S. and Marumo, F. (1996) Structure of aquaporin-2 vasopressin water channel. J. Biol. Chem. **271**, 5171–5176

28 Nour-Eldin, H. H., Hansen, B. G., Norholm, M. H., Jensen, J. K. and Halkier, B. A. (2006) Advancing uracil-excision based cloning towards an ideal technique for cloning PCR fragments. Nucleic Acids Res. **34**, e122

29 Bienert, G. P., Bienert, M. D., Jahn, T. P., Boutry, M. and Chaumont, F. (2011) Solanaceae XIPs are plasma membrane aquaporins that facilitate the transport of many uncharged substrates. Plant J. **66**, 306–317

30 Thompson, J. D., Higgins, D. G. and Gibson, T. J. (1994) CLUSTAL W: improving the sensitivity of progressive multiple sequence alignment through sequence weighting, position-specific gap penalties and weight matrix choice. Nucleic Acids Res. **22**, 4673–4680

31 Eswar, N., Webb, B., Marti-Renom, M. A., Madhusudhan, M. S., Eramian, D., Shen, M. Y., Pieper, U. and Sali, A. (2006) Comparative protein structure modeling using Modeller. Curr. Protoc. Bioinf. **15**, 5.6.1–5.6.30

32 Pierce, B. and Weng, Z. (2007) ZRANK: reranking protein docking predictions with an optimized energy function. Proteins **67**, 1078–1086

33 Zhou, H. and Zhou, Y. (2002) Distance-scaled, finite ideal-gas reference state improves structure-derived potentials of mean force for structure selection and stability prediction. Protein Sci. **11**, 2714–2726

34 Sayers, L. G., Miyawaki, A., Muto, A., Takeshita, H., Yamamoto, A., Michikawa, T., Furuichi, T. and Mikoshiba, K. (1997) Intracellular targeting and homotetramer formation of a truncated inositol 1,4,5-trisphosphate receptor-green fluorescent protein chimera in *Xenopus laevis* oocytes: evidence for the involvement of the transmembrane spanning domain in endoplasmic reticulum targeting and homotetramer complex formation. Biochem. J. **323**, 273–280

35 Moshelion, M., Hachez, C., Ye, Q., Cavez, D., Bajji, M., Jung, R. and Chaumont, F. (2009) Membrane water permeability and aquaporin expression increase during growth of maize suspension cultured cells. Plant, Cell Environ. **32**, 1334–1345

36 Guibault, G. G. (1990) Practical Fluorescence. Marcel Dekker Inc, New York

37 Fouquaert, E., Peumans, W. J., Vandekerckhove, T. T., Ongenaert, M. and Van Damme, E. J. (2009) Proteins with an Euonymus lectin-like domain are ubiquitous in Embryophyta. BMC Plant Biol. **9**, 136

38 Lagree, V., Froger, A., Deschamps, S., Pellerin, I., Delamarche, C., Bonnec, G., Gouranton, J., Thomas, D. and Hubert, J. F. (1998) Oligomerization state of water channels and glycerol facilitators. Involvement of loop E. J. Biol. Chem. **273**, 33949–33953

39 Mulders, S. M., Rijss, J. P., Hartog, A., Bindels, R. J., van Os, C. H. and Deen, P. M. (1997) Importance of the mercury-sensitive cysteine on function and routing of AQP1 and AQP2 in oocytes. Am. J. Physiol. **273**, F451–F456

40 Fancy, D. A., Denison, C., Kim, K., Xie, Y., Holdeman, T., Amini, F. and Kodadek, T. (2000) Scope, limitations and mechanistic aspects of the photo-induced cross-linking of proteins by water-soluble metal complexes. Chem. Biol. **7**, 697–708

41 Cavez, D., Hachez, C. and Chaumont, F. (2009) Maize black Mexican sweet suspension cultured cells are a convenient tool for studying aquaporin activity and regulation. Plant Signal Behav. **4**, 890–892

42 Henzler, T., Ye, Q. and Steudle, E. (2004) Oxidative gating of water channels (aquaporins) in Chara by hydroxyl radicals. Plant, Cell Environ. **27**, 1184–1195

43 Tournaire-Roux, C., Sutka, M., Javot, H., Gout, E., Gerbeau, P., Luu, D. T., Bligny, R. and Maurel, C. (2003) Cytosolic pH regulates root water transport during anoxic stress through gating of aquaporins. Nature **425**, 393–397

44 Zelazny, E., Miecielica, U., Borst, J. W., Hemminga, M. A. and Chaumont, F. (2009) An N-terminal diacidic motif is required for the trafficking of maize aquaporins ZmPIP2;4 and ZmPIP2;5 to the plasma membrane. Plant J. **57**, 346–355

45 Barone, L. M., Shih, C. and Wasserman, B. P. (1997) Mercury-induced conformational changes and identification of conserved surface loops in plasma membrane aquaporins from higher plants. Topology of PMIP31 from *Beta vulgaris* L. J. Biol. Chem. **272**, 30672–30677

46 Otto, B., Uehlein, N., Sdorra, S., Fischer, M., Ayaz, M., Belastegui-Macadam, X., Heckwolf, M., Lachnit, M., Pede, N., Priem, N. et al. (2010) Aquaporin tetramer composition modifies the function of tobacco aquaporins. J. Biol. Chem. **285**, 31253–31260

47 Daniels, M. J., Mirkov, T. E. and Chrispeels, M. J. (1994) The plasma membrane of *Arabidopsis thaliana* contains a mercury-insensitive aquaporin that is a homolog of the tonoplast water channel protein TIP. Plant Physiol. **106**, 1325–1333

48 Verdoucq, L., Grondin, A. and Maurel, C. (2008) Structure–function analysis of plant aquaporin AtPIP2;1 gating by divalent cations and protons. Biochem. J. **415**, 409–416

49 Chen, Y. F., Gao, Z., Kerris, III, R. J., Wang, W., Binder, B. M. and Schaller, G. E. (2010) Ethylene receptors function as components of high-molecular-mass protein complexes in *Arabidopsis*. PLoS ONE **5**, e8640

50 Trivedi, M. V., Laurence, J. S. and Siahaan, T. J. (2009) The role of thiols and disulfides on protein stability. Curr. Protein Pept. Sci. **10**, 614–625

51 Veerappan, A., Cymer, F., Klein, N. and Schneider, D. (2011) The tetrameric α-helical membrane protein GlpF unfolds via a dimeric folding intermediate. Biochemistry **50**, 10223–10230

Received 23 September 2011/3 April 2012; accepted 17 April 2012
Published as BJ Immediate Publication 17 April 2012, doi:10.1042/BJ20111704

Biochem. J. (2012) **445**, 101–111 (Printed in Great Britain) doi:10.1042/BJ20111704

SUPPLEMENTARY ONLINE DATA

A conserved cysteine residue is involved in disulfide bond formation between plant plasma membrane aquaporin monomers

Gerd P. BIENERT*[1], Damien CAVEZ*[1], Arnaud BESSERER*, Marie C. BERNY*, Dimitri GILIS†, Marianne ROOMAN† and François CHAUMONT*[2]

*Institut des Sciences de la Vie, Université Catholique de Louvain, Croix du Sud, 4-L7.07.14, 1348 Louvain-la-Neuve, Belgium, and †Bioinformatique génomique et structurale, Université Libre de Bruxelles, 1050 Brussels, Belgium

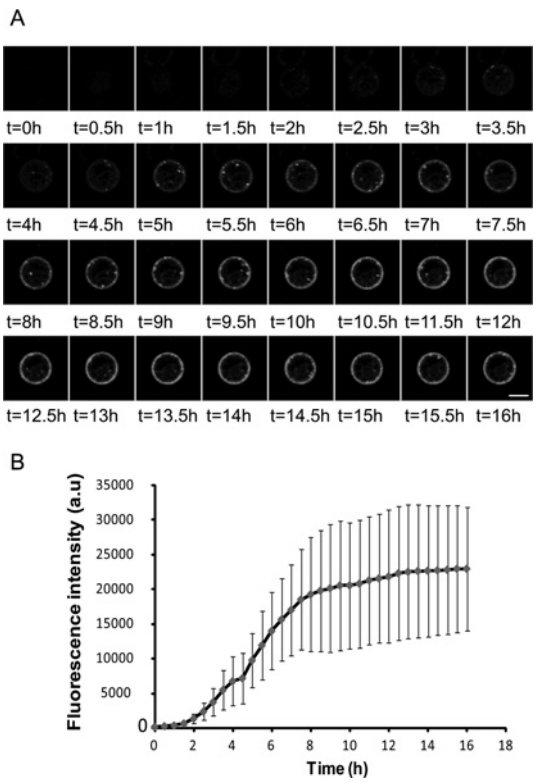

Figure S1 Expresion kinetics of mYFP–ZmPIP2;5 in maize mesophyll protoplasts

(**A**) Time-lapse fluorescence micrographs of a single optical slice in one maize mesophyll protoplast expressing mYFP–ZmPIP2;5. Immediately after protoplast transfection, a picture was taken every 30 min for 16 h using a confocal microscope. Scale bar = 10 μm. (**B**) Quantification of the total fluorescence intensity of protoplasts expressing mYFP–ZmPIP2;5 over time. Each time point is the mean of 20 independent measurements. Error bars show the 95 % confidence interval. a.u., absorbance units.

Received 23 September 2011/3 April 2012; accepted 17 April 2012
Published as BJ Immediate Publication 17 April 2012, doi:10.1042/BJ20111704

[1] Both of these authors contributed equally to this work.
[2] To whom correspondence should be addressed (email francois.chaumont@uclouvain.be).